

This discussion paper is/has been under review for the journal Hydrology and Earth System Sciences (HESS). Please refer to the corresponding final paper in HESS if available.

A comprehensive approach to analyze discrepancies between land surface models and in-situ measurements: a case study over US and Illinois with SECHIBA forced by NLDAS

M. Guimberteau¹, A. Perrier², K. Laval¹, and J. Polcher¹

¹Laboratoire de Météorologie Dynamique (LMD), UMR8539 – CNRS, Vincent Cassé, Palaiseau, 05: Ile-de-France Ouest et Nord, Paris, France

²AgroParisTech, UFR Physique de l'Environnement, Paris, France

Received: 2 March 2012 – Accepted: 10 April 2012 – Published: 18 April 2012

Correspondence to: M. Guimberteau (matthieu.guimberteau@upmc.fr)

Published by Copernicus Publications on behalf of the European Geosciences Union.

HESSD

9, 5039–5083, 2012

**SECHIBA forced by
NLDAS**

M. Guimberteau et al.

Title Page

Abstract

Introduction

Conclusions

References

Tables

Figures

◀

▶

◀

▶

Back

Close

Full Screen / Esc

Printer-friendly Version

Interactive Discussion



Abstract

The purpose of this study is to test the ability of the Land Surface Model SECHIBA to simulate water budget and particularly soil moisture at two different scales: regional and mesoscale. The model is forced by NLDAS data set at eighth degree resolution over the 1997–1999 period. SECHIBA gives satisfying results in terms of evapotranspiration and runoff over US compared with four other land surface models, all forced by NLDAS data set for a common time period. The simulated soil moisture is compared to in-situ data from the Global Soil Moisture Database across Illinois by computing a soil wetness index. A comprehensive approach is performed to test the ability of SECHIBA to simulate soil moisture with a gradual change of the vegetation parameters closely related to the experimental conditions. With default values of vegetation parameters, the model overestimates soil moisture, particularly during summer. Sensitivity tests of the model to the change of vegetation parameters are performed and show that the roots extraction parameter has the largest impact on soil moisture, others parameters such as LAI, height or soil resistance having a minor impact. Moreover, a new computation of evapotranspiration including bare soil evaporation under vegetation has been introduced into the model. The results point out an improvement of the simulation of soil moisture when this effect is taken into account. Finally, uncertainties in forcing precipitation to simulate a realistic soil moisture are addressed and it is shown that soil moisture observations can be rather different depending on the method to measure field capacity. When the observed field capacity is deducted from the observed volumetric water profiles, simulated soil wetness index is closer to the observations. Excepted for one station, the monthly mean correlation is around 0.9 between observation and simulation.

1 Introduction

Land Surface Models (LSMs) are designed to simulate surface conditions with vegetation and soil parameters that are calibrated at global scale. However, many studies

HESSD

9, 5039–5083, 2012

SECHIBA forced by NLDAS

M. Guimberteau et al.

Title Page

Abstract

Introduction

Conclusions

References

Tables

Figures

◀

▶

◀

▶

Back

Close

Full Screen / Esc

Printer-friendly Version

Interactive Discussion



focus on regional scale for model validation or climate change impacts. It is therefore reasonable to ask if the parameters of the LSMs are able to represent surface conditions in agreement with local measurements. Thus, a comprehensive approach is performed in this study focused on water budget simulation at large scale over the US and particularly on soil moisture content at regional scale over Illinois. Soil moisture is a crucial component of the water cycle. It strongly influences the partition of surface fluxes between latent and sensible heat. It impacts on evapotranspiration (ET) and consequently on the turbulent fluxes into the boundary layer and also on surface runoff. Findell and Eltahir (1997) found a correlation between an initial state of soil moisture at saturation and rainfall during summer studying observed data from Illinois. D'Odorico and Porporato (2004) showed a dependence between summer precipitation and antecedent soil moisture conditions. In climate simulations using LSM coupled to Global Circulation Model (GCM), the capture of the variation of soil moisture state during the year is important in order to have realistic feedback between continental surface and atmosphere. Much works have focused on the sensitivity of LSMs fluxes to soil moisture (Dirmeyer et al., 2000). The aim of this paper is to give an overview of the validity of three water cycle components simulated by the LSM SECHIBA (Schématisation des EChanges Hydriques à l'Interface Biosphère-Atmosphère, Ducoudré et al., 1993) at different spatial scales: ET, total runoff and soil moisture. Over the US, the first two are compared with results of LSMs forced by the same atmospheric forcing North American Land Data Assimilation System (NLDAS, Cosgrove et al., 2003) at eighth degree spatial resolution over 1997–1999 period. Then, we focus over a smaller region of the US, the state of Illinois, where in-situ soil moisture measurements have been performed and merged into a database by Robock et al. (2000). These observations are available for the studied time period (i.e. 1997–1999) and allow us to evaluate the SECHIBA results for simulated soil moisture. The ability of the LSM SECHIBA to simulate monthly variation of soil moisture is highlighted through a gradual and comprehensive adjustment of the parameters of the vegetation (LAI, root extraction, height). The impacts of the change of the parameters on simulated soil moisture are studied. Then, the

**SECHIBA forced by
NLDAS**

M. Guimberteau et al.

[Title Page](#)[Abstract](#)[Introduction](#)[Conclusions](#)[References](#)[Tables](#)[Figures](#)[◀](#)[▶](#)[◀](#)[▶](#)[Back](#)[Close](#)[Full Screen / Esc](#)[Printer-friendly Version](#)[Interactive Discussion](#)

uncertainties of dataset to assess the validity of the simulation are analysed. The role of precipitation rate during the studied period but also the significance of defining field capacity are highlighted.

2 Forcing and model

2.1 NLDAS forcing data set

The atmospheric forcing data set NLDAS used to force the model covers all the United States and a part of Canada and Mexico. The time resolution is hourly and the latitude-longitude spatial resolution is of eighth degree which is quite high compared to the current forcing resolution for LSMs generally around half degree. This high resolution is useful to investigate land surface processes at regional scales with better confidence and it is therefore suitable for this study. NLDAS data set is a combination of Eta Data Assimilation System (EDAS) models outputs, observation-based precipitation and shortwave radiation data. Precipitation forcing was built with Stage II hourly Doppler Radar and River Forecast Center gauge data (Baldwin and Mitchell, 1997), Climate Prediction Center (CPC) daily gauge data (Higgins et al., 2000) and reprocessed daily gauge data. Observed shortwave values are derived from Geostationary Operational Environmental Satellite (GOES) radiation data processed at the University of Maryland and at the National Environmental Satellite data and Information Service (Pinker et al., 2003). The nine primary forcing fields of the forcing used for this study are summed up in Table 1.

Precipitation is one of the most important forcing variables due to its strong impact on soil water budget and consequently on soil moisture content seasonality. In NLDAS, precipitation data comes from a combination of model outputs and observations. Therefore, differences can be found with in-situ data results which can be important for regional scale simulations. In this study, NLDAS precipitation is compared with in-situ observations from 16 Illinois Climate Network (ICN) stations averaged over Illinois,

SECHIBA forced by NLDAS

M. Guimberteau et al.

Title Page

Abstract

Introduction

Conclusions

References

Tables

Figures

◀

▶

◀

▶

Back

Close

Full Screen / Esc

Printer-friendly Version

Interactive Discussion



during the time period 1997–1999. The mean annual value of NLDAS precipitation is 2.73 mm d^{-1} over the period, 12 % higher than observations (2.44 mm d^{-1}). The highest overestimation occurs during spring and early summer (Fig. 1a). The overestimation is quasi-systematic during all the three years (Fig. 1b). However, NLDAS rainfall variation is quite satisfying (linear correlation is about 0.97) where the wet summer in 1998 and the dry autumn in 1999 are well captured.

2.2 Model description

SECHIBA is the hydrological module of the LSM ORCHIDEE (ORganising Carbon and Hydrology In Dynamic EcosystEMs), a model of the Pierre Simon Laplace Institute (IPSL), used to simulate the hydrological exchanges between soil, vegetation and atmosphere at a time-step of $\Delta t = 30 \text{ min}$.

2.2.1 Vegetation and LAI

In each grid-cell, up to thirteen Plant Functional Types (PFTs) can be represented simultaneously (including bare soil), prescribed by a vegetation map (International Geosphere Biosphere Programme (IGBP), Belward et al., 1999) according to the Olson classification (Olson et al., 1983). Maximal fraction of vegetation ν (f_ν^{\max}) is thus defined for each grid cell. It is modulated by the Leaf Area Index (LAI_ν) growth, specific for each PFT represented in the model, giving the fraction of vegetation f_ν :

$$f_\nu = f_\nu^{\max} \min(2\text{LAI}_\nu, 1) \quad (1)$$

The fraction of bare soil ($\nu = 1$) increases linearly as much as the decrease of the other fractions of vegetation ($2 \leq \nu \leq 13$) with a LAI lower than 0.5:

$$f_1 = f_1^{\max} + \sum_{\nu=2}^{13} (f_\nu^{\max} - f_\nu) \quad (2)$$

where f_1^{\max} is the maximal fraction of bare soil.

Title Page

Abstract

Introduction

Conclusions

References

Tables

Figures

◀

▶

◀

▶

Back

Close

Full Screen / Esc

Printer-friendly Version

Interactive Discussion



SECHIBA forced by
NLDAS

M. Guimberteau et al.

Title Page

Abstract

Introduction

Conclusions

References

Tables

Figures

◀

▶

◀

▶

Back

Close

Full Screen / Esc

Printer-friendly Version

Interactive Discussion



The choice between two methods for LAI parametrization is available in the model. It can be prescribed to the model by a map (Belward et al., 1999) whose values come from Normalized Difference Vegetation Index (NDVI) observations. The second method is the diagnostic computation of the LAI depending on the variation of soil temperature at 50 cm depth (T_{soil} in K) (Polcher, 1994). Temperature at this depth has a smoothed seasonality during the year and it is therefore adapted for LAI. This parametrization has been recently used in the model for a better seasonality of LAI for numerical experiments which simulates irrigation with SECHIBA (Guimberteau, 2006, 2010) and this method has been selected for our study. LAI growth is bounded by a minimal ($\text{LAI}_V^{\text{min}}$) and a maximal value ($\text{LAI}_V^{\text{max}}$) of LAI. Between these limits, LAI growth depends on the variation of soil temperature at 50 cm depth during the year, bounded by minimal ($T_{\text{soil}_V}^{\text{min}}$) and maximal values ($T_{\text{soil}_V}^{\text{max}}$) of soil temperature at 50 cm depth (both in K) that can be different according to the PFT considered (Guimberteau, 2006, 2010):

$$\text{LAI}_V = \text{LAI}_V^{\text{min}} + f(T_{\text{soil}_V}) (\text{LAI}_V^{\text{max}} - \text{LAI}_V^{\text{min}}) \quad (3)$$

where $f(T_{\text{soil}_V})$ (in K) is the function of growth of LAI for the PFT according to the soil temperature at 50 cm depth:

$$f(T_{\text{soil}_V}) = \left[1 - \left(\frac{T_{\text{soil}_V}^{\text{max}} - T_{\text{soil}}}{T_{\text{soil}_V}^{\text{max}} - T_{\text{soil}_V}^{\text{min}}} \right)^2 \right] \quad (4)$$

2.2.2 Soil hydrology

The hydrological model of Choisnel is used in SECHIBA for this study. The two meters ($h_{\text{tot}} = 2\text{m}$) soil column is represented by two moisture layers, a superficial one and a deep one (Fig. 2). The first layer has a thickness smaller than the lowest one

and its height h_{upper} (m) varies because it interacts strongly with the atmosphere. Consequently, the soil moisture of the superficial layer q_{upper} is directly controlled by the moisture convergence:

$$\frac{d}{dt}q_{\text{upper}} = P - E - D \quad (5)$$

where q_{upper} (kg m^{-2}) is the amount of water in the upper reservoir, $P = \text{Rainf} + \text{Snowf}$ ($\text{kg m}^{-2} \text{s}^{-1}$) is precipitation, E ($\text{kg m}^{-2} \text{s}^{-1}$) the total ET (that is to say the sum of water loss through bare soil evaporation, evaporation of water intercepted by the vegetation, transpiration of the cover and sublimation), and D ($\text{kg m}^{-2} \text{s}^{-1}$) the drainage between the two soil layers.

The hydrological budget is computed for each PFT within the mesh and then averaged over the grid cell. With this bucket model, we assume that surface runoff and deep drainage are produced only when soil reaches field capacity (when $q_{\text{upper}} + q_{\text{lower}} > q_{\text{tot}}$ where q_{tot} (kg m^{-2}) is the maximum amount of water that vegetation can extract from the soil). In the model, the total water excess is prescribed as: 95% in deep drainage ($\text{kg m}^{-2} \text{s}^{-1}$) and 5% in surface runoff R ($\text{kg m}^{-2} \text{s}^{-1}$). This hydrological scheme is described in detailed in Ducoudré et al. (1993) and D'Orgeval (2006).

The Soil Wetness Index (SWI) is used to describe the state of soil moisture and is useful to compare the different LSMs outputs (Dirmeyer et al., 2000) but also in-situ observations (Saleem and Salvucci, 2002). This index presented here is used in our study to compare SECHIBA outputs and observations data. SWI gives a simple representation of the water stress for the vegetation and indicates the actual available soil water for plants at each time. SWI ranges between 0 (lower this value, no more soil water can be extracted by the roots) to 1 (upper this value, no more water can be retained by the soil over some days):

$$\text{SWI} = \frac{W - W_{\text{wilt}}}{W_{\text{fc}} - W_{\text{wilt}}} \quad (6)$$

SECHIBA forced by NLDAS

M. Guimberteau et al.

Title Page

Abstract

Introduction

Conclusions

References

Tables

Figures

◀

▶

◀

▶

Back

Close

Full Screen / Esc

Printer-friendly Version

Interactive Discussion



where W (kg m^{-2}) is the actual equivalent water depth stored in the soil, W_{wilt} (kg m^{-2}) the equivalent water depth at the wilting point of the soil (determined by the soil and the vegetation properties) and W_{fc} (kg m^{-2}) the field capacity (based on soil texture alone) which represents the retained water in a natural soil after gravitation action.

The simulated SWI can be computed from the weighted average of the composite amount of water into each PFT reservoir:

$$\text{SWI}_{\text{ORCH}} = \frac{q_{\text{upper}} + q_{\text{lower}}}{q_{\text{tot}}} \quad (7)$$

where q_{tot} is obtained by integrating the maximal soil water amount per unit of soil volume ($w_{\text{max}} = 150 \text{ kg m}^{-3}$):

$$q_{\text{tot}} = h_{\text{tot}} w_{\text{max}} \quad (8)$$

The soil texture map of Zobler (1986) at a spatial resolution of $0.5^\circ \times 0.5^\circ$ is prescribed to the model. It is derived from the FAO soil data set (FAO, 1991).

2.2.3 Evapotranspiration and root extraction

ET is a sum of four components: evaporation of water intercepted by the cover (l_v in $\text{kg m}^{-2} \text{ s}^{-1}$), transpiration of vegetation (T_v in $\text{kg m}^{-2} \text{ s}^{-1}$), bare soil evaporation (E_1 in $\text{kg m}^{-2} \text{ s}^{-1}$), and sublimation of snow (not detailed here). In the initial version of SECHIBA (version HEAD 2007–2008), evaporation of water intercepted by the cover (Eq. 9) is computed only on the wet fraction $\frac{q'_v}{q'_v{}^{\text{max}}}$ and transpiration (T_v^{old} , Eq. 10) on the dry fraction of the leaves surfaces $\left(1 - \frac{q'_v}{q'_v{}^{\text{max}}}\right)$.

$$l_v = \min \left[q_v, f_v \frac{q'_v}{q'_v{}^{\text{max}}} \frac{1}{1 + \frac{r_{\text{sv}}}{r_a}} E_{\text{pot}} \right] = \min \left[q_v, l_v^{\text{max}} \right] \quad (9)$$

5046

Title Page

Abstract

Introduction

Conclusions

References

Tables

Figures

◀

▶

◀

▶

Back

Close

Full Screen / Esc

Printer-friendly Version

Interactive Discussion



where $q_v = f_v \cdot P$ ($\text{kg m}^{-2} \text{s}^{-1}$) is the flux of water intercepted by the cover, $q'_v = f_v P \Delta t$ (kg m^{-2}) is the amount of water (precipitation P) received by the leaf, $q_v^{\text{max}} = f_v \text{LAI}_v q_{\text{cst}}$ (kg m^{-2}) the maximal amount of intercepted water (where $q_{\text{cst}} = 0.1$ is the interception loss reservoir coefficient to convert leaf area index into size of interception loss reservoir), r_{sv} (s m^{-1}) the structural (or architectural) resistance, r_a (s m^{-1}) the aerodynamic resistance, E_{pot} ($\text{kg m}^{-2} \text{s}^{-1}$) the potential evaporation and l_v^{max} ($\text{kg m}^{-2} \text{s}^{-1}$) the maximal evaporation of water intercepted by the cover.

$$T_v^{\text{old}} = f_v \left(1 - \frac{q'_v}{q_v^{\text{max}}} \right) \left(\frac{1}{1 + \frac{r_{\text{sv}} + r_{\text{sto}_v}}{r_a}} \right) U_{\text{sv}} E_{\text{pot}} \quad (10)$$

where r_{sto_v} (s m^{-1}) is the canopy resistance (including both bulk stomatal and leaf aerodynamic resistances) and U_{sv} the root extraction potential (De Rosnay and Polcher, 1998) which reproduces the ability of roots to extract water (detailed next).

Bare soil evaporation (E_1^{old}) is computed through a resistance proportional to the relative dryness of the upper soil layer $h_{\text{upper}_1}^{\text{dry}}$ (m):

$$E_1^{\text{old}} = f_1 \frac{1}{1 + \frac{r_1}{r_a}} U_{\text{s}_1} E_{\text{pot}} \quad (11)$$

where r_1 (s m^{-1}) is the resistance to bare soil evaporation:

$$r_1 = h_{\text{upper}_1}^{\text{dry}} r_{\text{soil}} \quad (12)$$

where r_{soil} (s m^{-1}) is the resistance per dry soil meter. Initially, it is equal to 33000 s m^{-2} as introduced by Ducoudré et al. (1993).

According to Boone et al. (2004), ET simulated by SECHIBA is underestimated compared with other LSMs and especially bare soil evaporation component. Therefore,

SECHIBA forced by NLDAS

M. Guimberteau et al.

Title Page

Abstract

Introduction

Conclusions

References

Tables

Figures

◀

▶

◀

▶

Back

Close

Full Screen / Esc

Printer-friendly Version

Interactive Discussion



a new parametrization was implemented by D'Orgeval (2006) in the computation of water fluxes between soil, vegetation and atmosphere. The evaporation of water intercepted by the cover is now computed over the total surface of the leaf. In a first approximation, each time the potential flux is not satisfied by evaporation of intercepted water, the transpiration of the vegetation takes over (Eq. 13). It is constant as long as the sum of transpiration and evaporation of intercepted water is lower than potential evaporation.

$$T_v = \min \left[(I_v^{\max} - I_v), f_v \frac{1}{1 + \frac{r_{sv} + r_{sto_v}}{r_a}} U_{s_v} E_{\text{pot}} \right] \quad (13)$$

By this way, the sum of the evaporation of water intercepted by the leaves and the transpiration reaches faster the potential than in the previous parametrization. The total ET is consequently enhanced. Furthermore, the bare soil evaporation is computed more realistically because a sub-fraction of bare soil uncovered by the vegetation f_v^1 is estimated by an extinction coefficient $e = 0.5$:

$$f_v^1 = \exp(-eLAI_v) \quad (14)$$

This sub-fraction will increase with the decrease of the LAI typically in autumn and consequently enables the evaporation of the bare soil under vegetation. A new fraction of bare soil f_1' is defined in the model:

$$f_1' = \sum_{v=1}^{13} f_v^1 f_v \quad (15)$$

The bare soil evaporation is now computed over this new fraction:

$$E_1 = \min \left[f_1' E_1^{\text{old}}, E_{\text{pot}} - \sum_{v=2}^{13} (I_v + T_v) \right] \quad (16)$$

SECHIBA forced by NLDAS

M. Guimberteau et al.

Title Page

Abstract

Introduction

Conclusions

References

Tables

Figures

◀

▶

◀

▶

Back

Close

Full Screen / Esc

Printer-friendly Version

Interactive Discussion



SECHIBA forced by
NLDAS

M. Guimberteau et al.

Title Page

Abstract

Introduction

Conclusions

References

Tables

Figures

I◀

▶I

◀

▶

Back

Close

Full Screen / Esc

Printer-friendly Version

Interactive Discussion



Transpiration of the cover is governed by the ability of the roots to extract water from the soil (Desborough, 1997). This phenomenon is represented by the term U_{S_v} in equations of ET (De Rosnay and Polcher, 1998). It decreases exponentially when dry soil depth increases in order to represent the potential of water extraction by the roots (Fig. 3). It is more or less significant according to the dry soil depth. When it rains, the superficial layer of the soil can be saturated and no dry soil layer is present: $h_{\text{upper}_v}^{\text{dry}} = 0$ m and $U_{S_v} = 1$. ET is consequently maximal (at the potential value weighted by a term of resistance) and the roots are more efficient in extracting water for transpiration. On the contrary, under dry conditions, the layer of dry soil $h_{\text{upper}_v}^{\text{dry}}$ is formed and increases while U_{S_v} decreases exponentially approaching 0. The model simulates the difficulty for the roots to extract water all the more their density is low. In order to simulate the different intensity to extract water according to the PFT, different values of the parameter c_v have been attributed for each one. Therefore, a water extraction potential of roots U_{S_v} is computed for each PFT and for each soil layer. Two cases can be distinguished:

1. if the superficial reservoir of the soil does not exist, there is only one root extraction potential (Eq. 17)
2. if the superficial reservoir of the soil is present, one root extraction potential is distinguished for each reservoir (Eqs. 17 and 18) and the maximum between both is taken (Eq. 19). By this way, we favour the evaporation by the upper part of the root system whose efficiency in contributing water to transpiration is higher than lower roots (De Rosnay and Polcher, 1998).

$$U_{S_v}^{\text{lower}} = \exp \left(-c_v h_{\text{tot}} \frac{h_{\text{lower}_v}^{\text{dry}}}{h_{\text{tot}}} \right) \quad (17)$$

$$U_{s_v}^{\text{upper}} = \exp \left(-c_v h_{\text{tot}} \frac{h_{\text{upper},v}^{\text{dry}}}{h_{\text{upper},v}} \right) \quad (18)$$

$$U_{s_v} = \max \left(U_{s_v}^{\text{lower}}, U_{s_v}^{\text{upper}} \right) \quad (19)$$

2.3 Experimental design

The ability of the model SECHIBA to compute the water budget realistically at two different spatial scales is tested. In a first time, simulations with SECHIBA are performed over the US (Sect. 3.1) where mean annual ET (from initial computation in the model) and total runoff results are compared with four LSMs (NOAH, VIC, MOSAIC and SAC), during the numerical experiments performed in Mitchell et al. (2004). The simulations by the five models including SECHIBA have been performed over the time period 1st October 1997 to 30 September 1999 with the same forcing NLDAS.

In a second time, the study is focused on the Illinois state where measurements of soil moisture content were initiated by the Illinois Water Survey (Hollinger and Isard, 1994). These data is part of the Global Soil Moisture Database (Robock et al., 2000) which collect up to 15 yr in-situ recordings of soil moisture over more than 600 stations of many countries (such as Russia, China, Mongolia, India and USA). Simulated soil moisture content is compared with in-situ observations over 1997–1999 period (Sect. 3.2). The measurements were performed with neutron probes, first at eight grass-covered sites in 1981 and then seven sites were added in 1982 and two more in 1986. Finally, since 1992, nineteen ICN stations (see Table A1 in Appendix) have collected data especially soil moisture and precipitation. Soil moisture measurements were established on eighteen grass-covered stations and one on bare soil over the time period 1981–2004. They were taken within 11 soil layers to a depth of two meters; the first in the top 0.1 m of the profile, then every 0.2 m from a depth of 0.1 m

Title Page

Abstract

Introduction

Conclusions

References

Tables

Figures

◀

▶

◀

▶

Back

Close

Full Screen / Esc

Printer-friendly Version

Interactive Discussion



through 1.9 m, and the last in the layer between 1.9 m and 2.0 m. Each site was visited twice each month: the week of the 15th and the week of the last day of the month during March through September, and once each month during the last week of October through February (Hollinger and Isard, 1994). Excepted sand site at Topeka, silty loam (or silty clay loam for De Kalb and Champaign sites) is the predominant soil texture. In SECHIBA simulations, the texture of the soil is medium loam over Illinois. The impact of the difference in soil texture between simulation and observation on soil moisture content has not been tested in this study. One measurement station is associated with the corresponding grid cell of the model, according to the coordinate of the station (see Table A1 in Appendix) as in Fig. 4. For our study, each grid cell should be covered by only one PFT (grassland type) for an uniform parametrization. However, Fig. 4 a shows that few grid cells are covered by grassland (grid cells containing stations 9, 11 and 82). Moreover, less than 10 % of their area is covered by this PFT. The prevailing type of vegetation over Illinois in the model is the PFT “C₃ crops” type. Eight grid cells containing stations are covered by the PFT “C₃ crops” at least by 90 % (no. 1, 5, 6, 8, 9, 13, 15 and 16) according to Fig. 4b.

For the control simulation (SECH1) over Illinois, the computation of ET and the parametrization of the vegetation are those used for the study over US. First, gradual changes of crops parameters (LAI_v^{max} (SECH2), root extraction parameter c_v and crop height (SECH3), prescription of PFT “C₃ crops” over all the grid cells (SECH4)) and a test of the new ET computation (see Sect. 2.2.3, SECH5) are performed to be closely related to the experimental conditions over a grass cover. At each step, the accuracy to simulate more realistically the SWI seasonal variation is highlighted. Secondly, the uncertainties in forcing datasets such as precipitation input (SECH6) and their impact on simulated soil moisture content are studied. Moreover, we give a different method to deduct measured field capacity and show its impact on observed SWI computation. Thirdly, a comparison of the total runoff simulated by the model with data over the Kaskaskia River basin in Illinois is performed.

**SECHIBA forced by
NLDAS**

M. Guimberteau et al.

Title Page

Abstract

Introduction

Conclusions

References

Tables

Figures

◀

▶

◀

▶

Back

Close

Full Screen / Esc

Printer-friendly Version

Interactive Discussion



3 Results and discussion

3.1 Water balance simulated over US

According to Fig. 5, all the five models simulate the strong contrast between dried Western US where annual ET rate is generally less than 400 mm yr^{-1} , and humid Eastern US where annual ET rate is able to reach 800 mm yr^{-1} and more. However, different patterns are simulated according the models. The patterns are similar over western region (excepted over California) between the models but differences in ET rate are shown between VIC and SAC or MOSAIC of about 100 % over Eastern US. SECHIBA simulates an ET similar to NOAH, the values being often between 600 mm yr^{-1} and 800 mm yr^{-1} over Eastern US for these two particular models. To establish the validity of the results, Mitchell et al. (2004) have used observed streamflow and annual discharges from 1145 basins and converted (using the basin area) to area-average mean annual runoff. They showed that mean annual runoff simulated by NOAH was in good agreement with runoff data over southern and northern part of Eastern US. Consequently, we conclude that ET rate simulated by NOAH is satisfying whereas VIC underestimates it (and overestimates runoff), contrary to MOSAIC and SAC which overestimate it. The fact that, over this region, ET rate distribution obtained with SECHIBA is similar to NOAH results is rather encouraging. Considering more precisely the Southeastern US region, we notice however that the ET rates simulated with SECHIBA are larger than with NOAH along the coast. This might be an improvement: actually, the study conducted by Mitchell et al. (2004) seems to show an overestimation of annual runoff and consequently an underestimation of ET rate. This difference is also found between NOAH and SECHIBA results over some parts of Northeast US, although SECHIBA remains more similar to NOAH than to the three other models. Moreover, according to Mitchell et al. (2004), NOAH and VIC overestimate the runoff rate over the state of Illinois (excepted for extreme northeast), the values being between 400 and 500 mm yr^{-1} , whereas MOSAIC and SAC underestimate Illinois runoff (between 100 and 200 mm yr^{-1}). It is quite satisfying that SECHIBA gives an intermediate runoff of about $300\text{--}400 \text{ mm yr}^{-1}$ (not

Title Page

Abstract

Introduction

Conclusions

References

Tables

Figures

◀

▶

◀

▶

Back

Close

Full Screen / Esc

Printer-friendly Version

Interactive Discussion



shown) compared to the other models. Orders of magnitude of ET and runoff simulated by SECHIBA seems to be satisfactory over United States and particularly in Illinois. In order to evaluate soil moisture, a focus of the study is performed on this state where many observations are available.

3.2 Soil moisture simulated over Illinois

3.2.1 Progressive and comprehensive adjustments of vegetation parameters

The comparison of the SWI between simulation and observation is first performed over the eight grid cells mentioned in Sect. 2.3. Over Illinois, the mean SWI computed from observed soil moisture (hereafter called “SWI_o”) at 8 stations (Observations 8s) shows a pronounced seasonality during the year according to Fig. 6a. It is maximal during winter and early spring reaching 0.80 in March during the period of low ET. The SWI_o is decreasing during vegetation growth in spring to the middle of summer when climatic demand is maximal and thus water uptake by the vegetation significant. The SWI_o remains low during autumn with values around 0.40. It shows a high variation during the three years in average over Illinois where a dry event occurs during the autumn 1999 and the SWI_o value is less than 0.20 in November (Fig. 6b). This is due to the low precipitation occurring during this period over Illinois (less than 0.5 mm d^{-1} in November according to Fig. 1b). SECHIBA does not reproduce the soil moisture seasonality when initial values of the vegetation parameters are used (SECH1 simulation). The soil is almost saturated throughout the year even during summer months where a decrease of only 10 % is simulated (Fig. 6a). SECHIBA does not capture well the amplitude of soil moisture variations with a variance (3.77×10^{-3}) largely underestimated compared to observations (29.1×10^{-3}). However, a seasonal variation is already noticed in agreement with observations (Fig. 6b). These remarks are confirmed over each of the eight grid cells (not shown).

Different hypothesis that could explain the global overestimation of the simulated SWI are successively highlighted and tested in this study. The parameters of vegetation of

Title Page

Abstract

Introduction

Conclusions

References

Tables

Figures

◀

▶

◀

▶

Back

Close

Full Screen / Esc

Printer-friendly Version

Interactive Discussion



the model are gradually changed to be closer to the experimental conditions. First, the parametrization of LAI is changed through two modifications (SECH2 simulation). The maximum value of LAI initially equal to 2.0 is increased to 3.5 which corresponds to a very high maximal value of LAI for grassland. Specific values of soil temperature determining the seasonality of the LAI are now included as described in Sect. 2.2.1. We obtain a seasonal variation of LAI closer to a grass cover expected in such a temperate region like Illinois: values are around zero during winter whereas LAI increases rapidly during April to reach maximal values in summer and early autumn (Fig. 7). The change of the minimum value of LAI was also tested but had no significant impact on soil moisture (not shown). In fact, during winter, ET is strictly limited by the amount of incident energy and not by the cover of vegetation. The effect of the LAI increase on soil moisture is not significant during winter (Fig. 6a) because the water uptake by the vegetation through transpiration is near zero and only bare soil evaporation is occurring in SECH2 simulation (see Fig. 8). A higher decrease in soil moisture content compared to simulation SECH1 is found during late spring (Fig. 6a) due to the enhanced transpiration of the cover starting from the period of the vegetation growth (up to about $+0.3\text{mm d}^{-1}$ in June for SECH2 compared to SECH1, not shown) converting more energy with a higher LAI. Moreover, plants intercept more precipitation (not shown). Thus, total ET is increased even more during summer but simulated SWI remains overestimated compared to observations with a mean relative error of variance greater than 80 %.

In order to improve the soil moisture seasonality and particularly its decrease during summer, the ability of the roots to extract the water from the soil is enhanced. Therefore, the parameter $c_v = 4.0\text{m}^{-1}$ is put to 1.0 (SECH3 simulation). The roots density is consequently increased allowing a higher transpiration (up to $+1.5\text{mm d}^{-1}$ in July compared to SECH2 according to Fig. 8). The significant effect of the roots on the transpiration corroborates the result of Feddes et al. (2001) who showed that transpiration is more sensitive to the moisture content of a densely rooted soil layer. Moreover, De Rosnay and Polcher (1998) conclude that taking into account root profiles

**SECHIBA forced by
NLDAS**

M. Guimberteau et al.

Title Page

Abstract

Introduction

Conclusions

References

Tables

Figures

◀

▶

◀

▶

Back

Close

Full Screen / Esc

Printer-friendly Version

Interactive Discussion



improves the representation of the seasonal cycle of transpiration. As a result, in our simulation, the roots have a strong impact on soil moisture content and improves the simulated SWI seasonal variation with a mean relative error of variance of 7%. SWI mainly decreases during the period of vegetation in summer and autumn (up to 37.5% in September compared to SECH2) (Fig. 6a). Simulated SWI is in better agreement with SWI_o during autumn for the years 1997 and 1998 whereas the high decrease observed in 1999 is not enough pronounced in SECH3 (Fig. 6b). The results obtained during the dry season are different depending on the station. For example, at station 9, the pronounced decrease of the simulated SWI during autumn with SECH3 simulation compared to SECH2, induces a better capture of the soil dryness during this season when compared to the SWI_o (Fig. 9a). However, the simulated seasonality is poorly represented due to the soil moisture overestimation during spring in both simulations. At station 16, a lower decrease of the simulated SWI during spring induces a better seasonality even a systematic overestimation of the simulated SWI throughout the year compared to the SWI_o (Fig. 9b).

The height of SECHIBA vegetation is reduced from 1m to 30 cm which is more realistic to represent a grass cover. It has a little effect on soil moisture during autumn (up to 6% of increase in October compared to SECH2, not shown) due to a slight decrease in ET (not shown), the surface of exchanges of the plant with its atmosphere being reduced.

No significant impact on soil moisture is found (up to about 3% of decrease in March compared to SECH2, not shown) when the resistance of bare soil evaporation is tested (by dividing r_{soil} per 100). The results are quite similar over all the grid cells studied (not shown). This test shows that a value of 300 s m^{-1} for the resistance is already large enough to simulate the decrease of bare soil evaporation when soil moisture is low. This is because SECHIBA simulates a low bare soil evaporation. For this reason, a new computation of the latter taking into account bare soil evaporation under the vegetation, is proposed in this study.

**SECHIBA forced by
NLDAS**

M. Guimberteau et al.

Title Page

Abstract

Introduction

Conclusions

References

Tables

Figures

◀

▶

◀

▶

Back

Close

Full Screen / Esc

Printer-friendly Version

Interactive Discussion



**SECHIBA forced by
NLDAS**

M. Guimberteau et al.

Title Page

Abstract

Introduction

Conclusions

References

Tables

Figures

◀

▶

◀

▶

Back

Close

Full Screen / Esc

Printer-friendly Version

Interactive Discussion



In conclusion, a grass cover rather realistic is thus modeled with simulation SECH3 where the maximum LAI is of 3.5 and the height of 30 cm. The sensitivity tests highlight the major impact of the roots extraction on soil moisture content in our model. The value of $c_v = 1.0\text{m}^{-1}$ allows more extraction of water from the first 50 cm of soil and soil moisture shows a higher decrease during spring and summer in agreement with reality. The other parameters as LAI and height of vegetation or soil resistance have a minor impact.

A new simulation is performed (SECH4 simulation) where the parametrization of vegetation in SECH3 is kept but the same PFT is setting everywhere on the grid cells of SECHIBA. This simulation is judicious as far as there is no feedback from the surface to the atmosphere. Thus, the impacts of the vegetation around the studied grid cells can be left. This allows us to include the results from all the grid cells containing the stations. When all the same type of vegetation is set across the model grid, simulated soil moisture content remains overestimated compared to the new average of observations (“Observations 17 s”) according to Fig. 10a. However, the seasonal variation is slightly improved compared to SECH3 with a mean relative error of variance of about 3.1 %. This improvement could be explained by the increase of the sampling improving the statistic for the simulation SECH4.

A new computation of ET which allows bare soil evaporation under the vegetation is implemented in SECHIBA (simulation SECH5). In this simulation, the parametrization of vegetation is the same than in SECH4. Global increase in ET simulated by SECH5 is low (+8.0%) compared to SECH4, in average over the stations. Bare soil evaporation is now simulated throughout the year with SECH5, even when vegetation is present during summer (Fig. 11). As long as the total available energy to evaporate do not change between the two simulations, the transpiration of the cover decreases (evaporation of water intercepted by the cover does not change significantly). The global increase in ET has a significant impact on soil moisture when SECH5 is compared to SECH4. This change improves the seasonality of soil moisture (Fig. 10a). A decrease in soil moisture occurs throughout the year and particularly during autumn (up to 16 % of decrease in

November). Simulated SWI is mainly improved compared to measurements during the autumn 1997 and 1998 whereas in autumn 1999 it remains overestimated (Fig. 10b).

Finally, the adjustment of the potential of water extraction by the roots and the implementation of the new computation of ET in the model are essential to simulate soil moisture in agreement with measurements at fine scale.

3.2.2 Uncertainties in rainfall forcing data

In order to test the uncertainty of the precipitation forcing, a substitution of the NLDAS precipitations by the in-situ observed precipitation data (see Sect. 2.1) has been performed for each station in the corresponding grid cell of the forcing grid. The impact on soil moisture is then studied with simulation SECH6 including parametrization of vegetation and ET computation used in SECH5. Mean annual SWI simulated by SECHIBA forced by in-situ precipitations is decreased compared to SECH5 (Fig. 12) where NLDAS precipitation is lower than in-situ measurements (see Sect. 2.1). However, the decrease of simulated SWI occurs only during summer and autumn where it is now in good agreement with the SWIo (Fig. 12a) and particularly for the year 1998 (Fig. 12b). The overestimation of simulated SWI during the autumn 1999 is greatly reduced when in-situ precipitations are used. It is closer to the measurements which pointed out more dryness of the soil than the two previous years at the same time period (Fig. 12b). During winter and spring, SWI simulated with SECH6 slightly increases compared to SECH5 and remains systematically overestimated compared to the SWIo (Fig. 12a).

3.2.3 A different method to get measured field capacity

The result of field capacity measurement can be slightly different whether it is performed in laboratory or in-situ. Field capacity is usually measured in laboratory using “a pressure plate to apply a suction of $-1/3$ atmosphere to a saturated soil sample. When water is no longer leaving the soil sample, the soil moisture in the sample is determined gravimetrically and equated to field capacity.” (Walker, 1989). Field method

SECHIBA forced by NLDAS

M. Guimberteau et al.

Title Page

Abstract

Introduction

Conclusions

References

Tables

Figures

◀

▶

◀

▶

Back

Close

Full Screen / Esc

Printer-friendly Version

Interactive Discussion



which consist in irrigating a test plot until the soil profile is saturated is particularly restrictive for this type of study. We suggest another method to measure the field capacity. It is considered as the maximal value of volumetric water in the soil during the year. Thus, we plot the monthly mean observed volumetric water profiles in average over the stations (Fig. 13) to deduce the field capacity: the maximal value of volumetric water during the year is obtained in March on the 30–50 cm layer of the soil (we consider that the 0–10 cm layer is not representative of the field capacity). This value deduced from the volumetric water profile (0.39 kg m^{-3}) is lower than the measured field capacity (0.41 kg m^{-3}). The SWlo is then recomputed with the new value of field capacity (corresponding to “Observations 17 sfc” in Fig. 14) and its seasonality is compared to SECH6. The decrease of the field capacity in the re-computed SWlo leads to an increase of the observed SWI particularly during winter and spring. The simulated SWI from SECH6 becomes consequently closer to the re-computed SWlo during the three years with a better similarity in amplitude of the seasonality (Fig. 14).

3.2.4 Global analyze

To summarize in detail our results with simulation SECH6, the amplitude and the phase of the simulated SWI seasonality are represented for each station of Illinois (triangle) in the Taylor diagram (Taylor, 2001) (Fig. 15). Overall, many stations show a simulated SWI in good agreement with the SWlo including field capacity correction when SECHIBA is forced with in-situ precipitation and parametrized according to SECH6. Less than the half of the stations presents a relative error of SWI with observations around 10 % and less. SECHIBA captures quite well the phase of the SWI seasonality over Illinois (more than 80 % of stations shows a correlation greater than 0.85). The amplitude of SWI, which is very different according to the station, is much harder to capture (about 50 % of stations have a standard deviation of more or less 0.25 comparing to unit). The interannual variation of the simulated SWI is compared with the SWlo throughout the three years at each station in Fig. A1 in Appendix. Seasonality of simulated SWI at station 10 is the closest to the SWlo in term of amplitude (ratio of

SECHIBA forced by NLDAS

M. Guimberteau et al.

Title Page

Abstract

Introduction

Conclusions

References

Tables

Figures

◀

▶

◀

▶

Back

Close

Full Screen / Esc

Printer-friendly Version

Interactive Discussion



standard deviation is close to 1), phase (0.98 of correlation) (Fig. 15) and magnitude (17.5% of relative error). SWI at station 13 is the worst simulated because of its low observed amplitude of SWI which SECHIBA cannot capture (Fig. A1).

3.2.5 Simulated total runoff

5 The resulting total runoff simulated with SECH6 is compared with Kaskaskia stream-flow data (divided by its corresponding basin surface) at Venedy station point (38°27' N; 89°37' W), obtained from United States Geological Survey (USGS) for the period 1997–1999. The watershed integrates a large part of runoff over the south-west of Illinois. Runoff simulated with SECH6 is underestimated by 24 %. However, during the first half
10 of the year, total runoff is well simulated (the mean relative error is about 2.5% for the period January–May). SECHIBA reaches to capture the peak of runoff observed in March (Fig. 16). During the rest of the year, the simulated total runoff is null leading an underestimation in average over the year. This is partly due to the parametrization of the hydrological model of Choisnel which cannot produce runoff and drainage as far
15 as simulated soil moisture does not reach field capacity. In the parametrization of the model used for simulation SECH6, the improvement of root extraction potential generates a level of soil moisture content always far from the field capacity during summer and consequently exacerbates the limitation of the Choisnel hydrological modelling to simulate total runoff. The use of a multilayer approach to represent the vertical soil
20 water diffusion (De Rosnay, 1999; De Rosnay et al., 2002) might be more satisfying to generate runoff and infiltration but it has not been tested in this study. However, underestimation of total runoff by SECHIBA can be due to the complexity of the water exchange between the deep soil and the surface through the water table that are included in the measurements datasets but not represented in the model.

SECHIBA forced by NLDAS

M. Guimberteau et al.

Title Page

Abstract

Introduction

Conclusions

References

Tables

Figures

◀

▶

◀

▶

Back

Close

Full Screen / Esc

Printer-friendly Version

Interactive Discussion



4 Conclusions

This paper investigated the ability of SECHIBA to compute the surface water balance at two different spatial scales. At large scale (over the United States), ET and total runoff results from SECHIBA, forced by NLDAS at eighth degree resolution, are in good agreement with NOAA, considered as the closest to observations. At regional scale (over Illinois), soil moisture content simulated by SECHIBA forced by the same dataset has been compared to observations from a global soil moisture database. When vegetation parameters are defined by experimental conditions, the model is able to capture rather well the seasonal variation of soil moisture. The magnitude, amplitude and phase are well reproduced by the model over many stations. Uncertainties in climatic data, such as precipitation, that can induce a bias in the simulations of soil moisture, have been also pointed out. Extensions of this study could be performed such as the use of the new hydrological module or the dynamical vegetation to improve the simulation of soil moisture content. Moreover, the study of the impact of soil texture on soil moisture content is a reliable perspective to extend this study. The improvement of spatial resolution is a big challenge for climate modelling and particularly for the LSM which simulates land-use change. In this study, it is rather encouraging to obtain a realistic soil moisture seasonality at fine scale over Illinois with a global model such as SECHIBA which includes the simple hydrological model of Choisnel. Impact studies on water resources can be addressed with more confidence since soil moisture which has a crucial impact on water cycle, is well represented. For example, Guimberteau et al. (2011) simulated with SECHIBA coupled with LMDZ (Laboratoire de Météorologie Dynamique Zoom, Hourdin et al., 2006) a significant decrease in precipitation due to irrigation over the eastern part of the Mississippi River basin. Our comprehensive approach of gradual changes of the vegetation parameters over Illinois which is part of this region, can lead to a better understanding in the processes between the irrigated vegetation cover and climate.

SECHIBA forced by NLDAS

M. Guimberteau et al.

Title Page

Abstract

Introduction

Conclusions

References

Tables

Figures

◀

▶

◀

▶

Back

Close

Full Screen / Esc

Printer-friendly Version

Interactive Discussion



Acknowledgements. We gratefully acknowledge Alan Robock to make available the soil moisture data bank of Illinois (Robock et al., 2000). We thank NLDAS team to make available NLDAS forcing datasets. We also thank the two scientific software engineers Martial Mancip and Patrick Brockmann (both IPSL) for their help about, respectively NLDAS forcing building for the SECHIBA model and for the fusion of the observed precipitation in NLDAS fields. Simulations have been performed using computational facilities of the Institut du Développement et des Ressources en Informatique Scientifique (IDRIS, CNRS, France).



The publication of this article is financed by CNRS-INSU.

References

- Baldwin, M. E. and Mitchell, K. E.: The NCEP hourly multi-sensor U.S. precipitation analysis for operations and GCIP research, Preprints, 13th Conference on Hydrology, Long Beach, CA, Am. Meteorol. Soc., 54–55, 1997. 5042
- Belward, A., Estes, J., and Kline, K.: The IGBP-DIS global 1-km land-cover data set DISCover: a project overview, Photogramm. Eng. Rem. S., 5(9), 1013–1020, 1999. 5043, 5044
- Boone, A., Habets, F., Noilhan, J., Clark, D., Dirmeyer, P., Fox, S., Gusev, Y., Haddeland, I., Koster, R., Lohmann, D., Mahanama, S., Mitchell, K., Nasonova, O., Niu, G.-Y., Pitman, A., Polcher, J., Shmakin, A. B., Tanaka, K., van den Hurk, B., Vérant, S., Verseghy, D., Viterbo, P., and Yang, Z.-L.: The Rhone-Aggregation land surface scheme intercomparison project: an overview, J. Climate, 17(1), 187–208, 2004. 5047
- Cosgrove, B., Lohmann, D., Mitchell, K., Houser, P., Wood, E., Schaake, J., Robock, A., Marshall, C., Sheffield, J., Qingyuan, D., Lifeng, L., Higgins, R., Pinker, R., Tarpley, J., and Meng, J.: Real-time and retrospective forcing in the North American Land Data Assimilation Sys-

HESSD

9, 5039–5083, 2012

SECHIBA forced by NLDAS

M. Guimberteau et al.

Title Page

Abstract

Introduction

Conclusions

References

Tables

Figures

◀

▶

◀

▶

Back

Close

Full Screen / Esc

Printer-friendly Version

Interactive Discussion



tem (NLDAS) project, *J. Geophys. Res.*, 108(D22), 8842, doi:10.1029/2002JD003118, 2003. 5041

De Rosnay, P.: Représentation de l'interaction sol-végétation-atmosphère dans le modèle de circulation générale du Laboratoire de Météorologie Dynamique thesis, State Univ. Pierre et Marie Curie, Paris VI, 176 pp., 1999. 5059

De Rosnay, P. and Polcher, J.: Modelling root water uptake in a complex land surface scheme coupled to a GCM, *Hydrol. Earth Syst. Sci.*, 2, 239–255, doi:10.5194/hess-2-239-1998, 1998. 5047, 5049, 5054, 5069

De Rosnay, P., Polcher, J., Bruen, M., and Laval, K.: Impact of a physically based soil water flow and soil-plant interaction representation for modeling large-scale land surface processes, *J. Geophys. Res.-Atmos.*, 107(D11), 4118, doi:10.1029/2001JD000634, 2002. 5059

Desborough, C.: The impact of root weighting on the response of transpiration to moisture stress in land surface schemes, *Mon. Weather Rev.*, 125(8), 1920–1930, 1997. 5049

Dirmeyer, P., Zeng, F., Ducharne, A., Morrill, J., and Koster, R.: The sensitivity of surface fluxes to soil water content in three land surface schemes, *J. Hydrometeorol.*, 1(2), 121–134, 2000. 5041, 5045

D'Odorico, P. and Porporato, A.: Preferential states in soil moisture and climate dynamics, *P. Natl. Acad. Sci.*, 101(24), 8848–8851, 2004. 5041

D'Orgeval, T.: Impact du changement climatique sur le cycle de l'eau en Afrique de l'Ouest: modélisation et incertitudes, PhD thesis, Université Paris VI, 2006. 5045, 5048

Ducoudré, N., Laval, K., and Perrier, A.: SECHIBA, a new set of parameterizations of the hydrologic exchanges at the land atmosphere interface within the LMD atmospheric global circulation model, *J. Climate*, 6(2), 248–273, 1993. 5041, 5045, 5047

FAO: The digitized soil map of the world (release 1.0), *World Soil Resour. Rep. 67/1*, FAO, Rome, 1991. 5046

Feddes, R., Hoff, H., Bruen, M., Dawson, T., De Rosnay, P., Dirmeyer, P., Jackson, R., Kabat, P., Kleidon, A., Lilly, A., and Pitman, A. J.: Modeling root water uptake in hydrological and climate models, *B. Am. Meteorol. Soc.*, 82(12), 2797–2810, 2001. 5054

Findell, K. and Eltahir, E.: An analysis of the soil moisture-rainfall feedback, based on direct observations from Illinois, *Water Resour. Res.*, 33(4), 725–735, 1997. 5041

Guimberteau, M.: Analyse et modifications proposées de la modélisation de l'irrigation dans un modèle de surface, Master's thesis, Université Pierre et Marie Curie Paris VI-Laboratoire de Météorologie Dynamique Paris Jussieu, 2006. 5044

HESD

9, 5039–5083, 2012

SECHIBA forced by NLDAS

M. Guimberteau et al.

Title Page

Abstract

Introduction

Conclusions

References

Tables

Figures

◀

▶

◀

▶

Back

Close

Full Screen / Esc

Printer-friendly Version

Interactive Discussion



- Guimberteau, M.: Modélisation de l'hydrologie continentale et influences de l'irrigation sur le cycle de l'eau, PhD thesis, Université Paris VI, 2010. 5044
- Guimberteau, M., Laval, K., Perrier, A., and Polcher, J.: Global effect of irrigation and its impact on the onset of the Indian summer monsoon, *Clim. Dynam.*, online first, doi:10.1007/s00382-011-1252-5, 2011. 5060
- Higgins, R., Shi, W., Yarosh, E., and Joyce, R.: Improved United States precipitation quality control system and analysis, NCEP/Climate Prediction Center Atlas, US Dept. of Commerce/Natl. Weather Serv. Natl. Oceanic and Atmos. Admin., Camp Springs, Md., 7, 40, 2000. 5042
- Hollinger, S. and Isard, S.: A soil-moisture climatology of Illinois, *J. Climate*, 7(5), 822–833, 1994. 5050, 5051
- Hourdin, F., Musat, I., Bony, S., Braconnot, P., Codron, F., Dufresne, J.-L., Fairhead, L., Filiberti, M.-A., Friedlingstein, P., Grandpeix, J.-Y., Krinner, G., LeVan, P., Li, Z.-X., and Lott, F.: The LMDZ4 general circulation model: climate performance and sensitivity to parametrized physics with emphasis on tropical convection, *Clim. Dynam.*, 27(7), 787–813, 2006. 5060
- Mitchell, K., Lohmann, D., Houser, P., Wood, E., Schaake, J., Robock, A., Cosgrove, B., Sheffield, J., Duan, Q., Luo, L., Higgins, R., Pinker, R., Tarpley, J., Lettenmaier, D., Marshall, C., Entin, J., Pan, M., Shi, W., Koren, V., Meng, J., Ramsay, B., and Bailey, A.: The multi-institution North American Land Data Assimilation System (NLDAS): utilizing multiple GCIP products and partners in a continental distributed hydrological modeling system, *J. Geophys. Res.-Atmos.*, 109(D7), D07S90, doi:10.1029/2003JD003823, 2004. 5050, 5052, 5071
- Olson, J., Watts, J., and Allison, L.: Carbon in Live Vegetation of Major World Ecosystems (ORNL-5862), Environmental Sciences Division Publication, Oak Ridge National Lab., TN (USA), 1983. 5043
- Pinker, R., Tarpley, J., Laszlo, I., Mitchell, K., Houser, P., Wood, E., Schaake, J., Robock, A., Lohmann, D., Cosgrove, B., Sheffield, J., Duan, Q., Luo, L., and Higgins, R.: Surface radiation budgets in support of the GEWEX Continental-Scale International Project (GCIP) and the GEWEX Americas Prediction Project (GAPP), including the North American Land Data Assimilation System (NLDAS) Project, *J. Geophys. Res.-Atmos.*, 108(D22), 8844, doi:10.1029/2002JD003301, 2003. 5042
- Polcher, J.: Etude de la sensibilité du climat tropical à la déforestation, Thèse de Doctorat, Univ. Pierre et Marie Curie, Paris, 1994. 5044

**SECHIBA forced by
NLDAS**

M. Guimberteau et al.

Title Page

Abstract

Introduction

Conclusions

References

Tables

Figures

◀

▶

◀

▶

Back

Close

Full Screen / Esc

Printer-friendly Version

Interactive Discussion



Robock, A., Vinnikov, K., Srinivasan, G., Entin, J., Hollinger, S., Speranskaya, N., Liu, S., and Namkhai, A.: The global soil moisture data bank, *B. Am. Meteorol. Soc.*, 81(6), 1281–1299, 2000. 5041, 5050, 5061

5 Saleem, J. and Salvucci, G.: Comparison of soil wetness indices for inducing functional similarity of hydrologic response across sites in Illinois, *J. Hydrometeorol.*, 3(1), 80–91, 2002. 5045

Taylor, K.: Summarizing multiple aspects of model performance in a single diagram, *J. Geophys. Res.-Atmos.*, 106(D7), 7183–7192, 2001. 5058

10 Walker, W.: Guidelines for designing and evaluating surface irrigation systems, FAO, Rome, 1989. 5057

Zobler, L.: A world soil file for global climate modeling, NASA technical memorandum, 87802(3), National Aeronautics and Space Administration. Washington, D.C., 1986. 5046

HESSD

9, 5039–5083, 2012

SECHIBA forced by NLDAS

M. Guimberteau et al.

Title Page

Abstract

Introduction

Conclusions

References

Tables

Figures

◀

▶

◀

▶

Back

Close

Full Screen / Esc

Printer-friendly Version

Interactive Discussion



SECHIBA forced by
NLDAS

M. Guimberteau et al.

Table 1. List of atmospheric forcing variables in NLDAS used for this study.

Name	Description	Units
T_{air}	Two meters air temperature	K
Q_{air}	Two meters air specific humidity	kg kg^{-1}
Wind_N	Ten meters wind speed (u component)	m s^{-1}
Wind_E	Ten meters wind speed (v component)	m s^{-1}
P_{surf}	Surface pressure	Pa
SW_{down}	Surface downward short wave flux	W m^{-2}
LW_{down}	Surface downward long wave flux	W m^{-2}
Rainf	Rainfall rate	$\text{kg m}^{-2} \text{s}^{-1}$
Snowf	Snowfall rate	$\text{kg m}^{-2} \text{s}^{-1}$

Title Page

Abstract

Introduction

Conclusions

References

Tables

Figures

I◀

▶I

◀

▶

Back

Close

Full Screen / Esc

Printer-friendly Version

Interactive Discussion



SECHIBA forced by
NLDAS

M. Guimberteau et al.

Table A1. List of measurements stations with their references (number, site code, coordinates and elevation). We do not take account the two following stations for the present study.

Number	Name	Site code	Latitude (N)	Longitude (W)	Elevation (m)
1	Bondville	BVL	40°03′	88°52′	213
2 ⁺ /82	Dixon Springs (bare ⁺ /grass)	DXG	37°27′	88°40′	165
3	Brownstown	BRW	38°57′	88°57′	177
4	Perry	ORR	39°48′	90°50′	206
5	De Kalb	DEK	41°51′	88°51′	265
6	Monmouth	MON	40°65′	90°41′	229
8	Peoria	ICC	40°42′	89°32′	207
9	Springfield	LLC	39°31′	89°37′	177
10	Belleville	FRM	38°31′	89°53′	133
11	Carbondale	SIU	37°43′	89°14′	137
12	Olney	OLN	38°44′	88°06′	134
13	Freeport	FRE	42°14′	89°40′	265
14	Ina	RND	38°08′	88°55′	130
15	Stelle	STE	40°25′	89°19′	207
16	Topeka	MTF	40°18′	89°54′	152
17 [*]	Oak Run [*]	OAK [*]	40°58′	90°09′	265
34	Fairfield	FAI	38°23′	88°23′	136
81	Champaign	CMI	40°07′	88°14′	219

* Missing data for 1998 and 1999 for this station

⁺ Measurements performed over bare soil for this station.

Title Page

Abstract

Introduction

Conclusions

References

Tables

Figures

I◀

▶I

◀

▶

Back

Close

Full Screen / Esc

Printer-friendly Version

Interactive Discussion



SECHIBA forced by
NLDAS

M. Guimberteau et al.

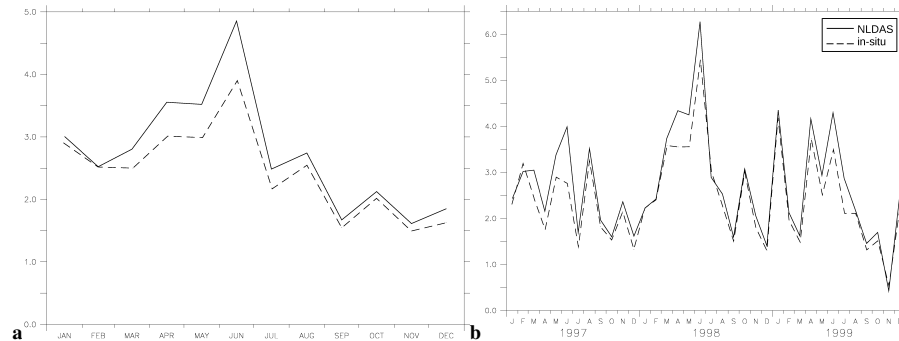


Fig. 1. (a) Seasonal cycles and (b) time series of monthly mean precipitation (mm d^{-1}) averaged over 16 stations across Illinois, from NLDAS forcing and in-situ observations, for the time period 1997–1999.

[Title Page](#)[Abstract](#)[Introduction](#)[Conclusions](#)[References](#)[Tables](#)[Figures](#)[I◀](#)[▶I](#)[◀](#)[▶](#)[Back](#)[Close](#)[Full Screen / Esc](#)[Printer-friendly Version](#)[Interactive Discussion](#)

SECHIBA forced by
NLDAS

M. Guimberteau et al.

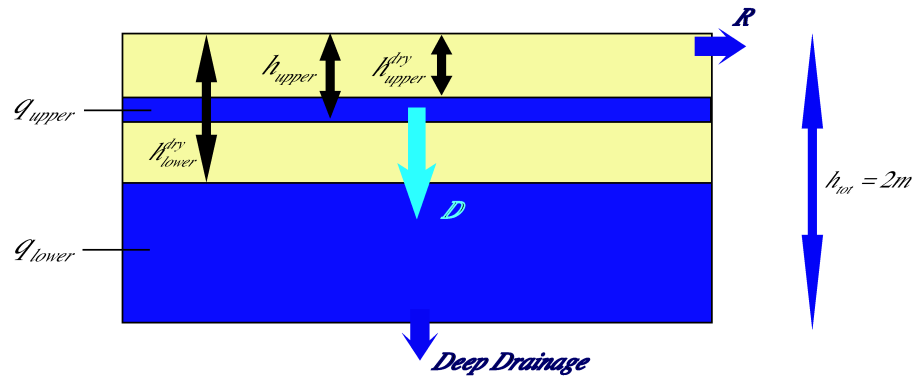


Fig. 2. Scheme of the soil with Choisnel hydrology in SECHIBA. q_{upper} and q_{lower} (both in kgm^{-2}) are, respectively the amount of water contained in the upper and lower reservoir, h_{upper}^{dry} and h_{lower}^{dry} (both in m) the depths of dry soil layers, respectively over the superficial and the deep soil reservoir, h_{upper} (m) is the height of the superficial reservoir, R the runoff at the surface and D ($\text{kgm}^{-2}\text{s}^{-1}$) the drainage between the two soil layers.

Title Page

Abstract

Introduction

Conclusions

References

Tables

Figures

◀

▶

◀

▶

Back

Close

Full Screen / Esc

Printer-friendly Version

Interactive Discussion



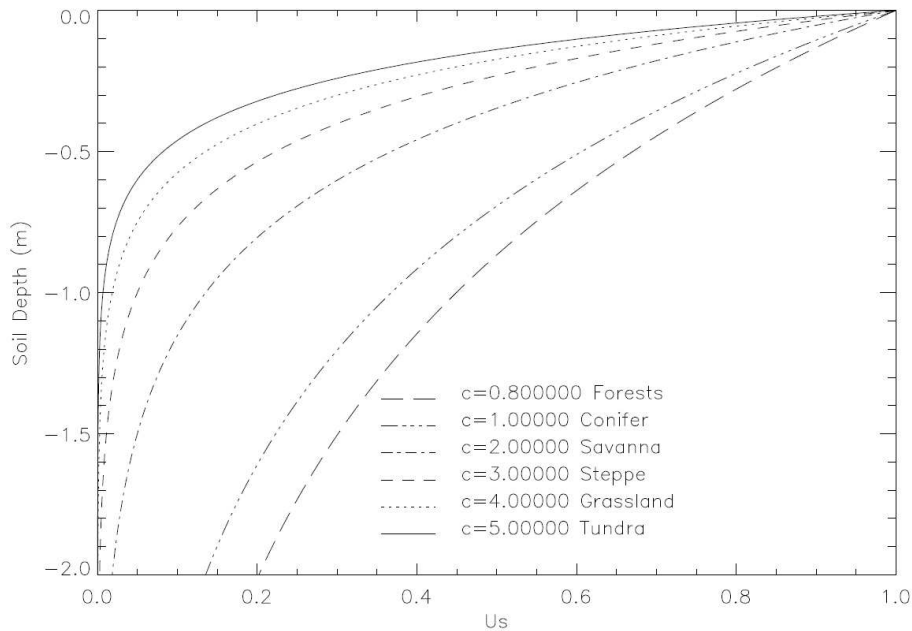


Fig. 3. Water uptake function, U_{s_v} , for each canopy (De Rosnay and Polcher, 1998). The profiles depend on the depth of the dry soil and the value of the constant c_v .

SECHIBA forced by NLDAS

M. Guimberteau et al.

Title Page

Abstract Introduction

Conclusions References

Tables Figures

◀ ▶

◀ ▶

Back Close

Full Screen / Esc

Printer-friendly Version

Interactive Discussion



SECHIBA forced by
NLDAS

M. Guimberteau et al.

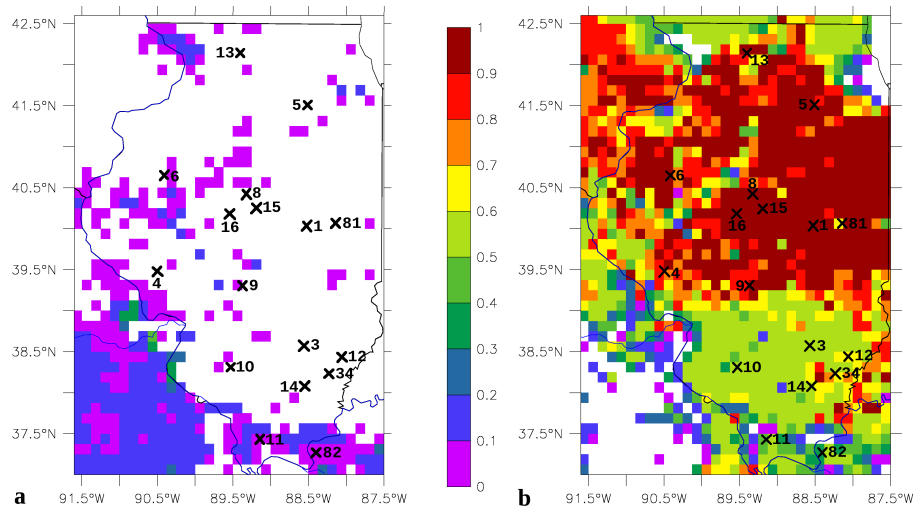


Fig. 4. Fraction of PFT (a) “ C_3 grassland” and (b) “ C_3 crops” covers on each grid cell across Illinois prescribed by the vegetation map in SECHIBA. The 17 stations used for this study are indicated on the figure (see Table A1 in Appendix for their references).

Title Page

Abstract

Introduction

Conclusions

References

Tables

Figures

I◀

▶I

◀

▶

Back

Close

Full Screen / Esc

Printer-friendly Version

Interactive Discussion



SECHIBA forced by
NLDAS

M. Guimberteau et al.

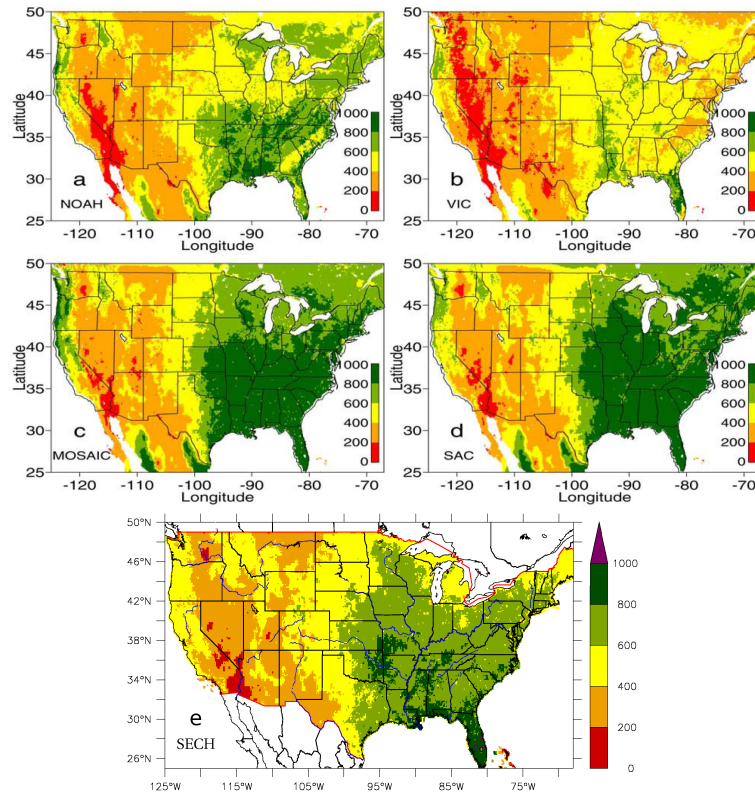


Fig. 5. Mean annual ET (mm yr^{-1}) over the United States, for the mean time period 1 October 1997–30 September 1999, from (a) NOAH, (b) VIC, (c) MOSAIC (d) SAC and (e) SECHIBA. The first four maps were taken from Mitchell et al. (2004).

[Title Page](#)[Abstract](#)[Introduction](#)[Conclusions](#)[References](#)[Tables](#)[Figures](#)[I◀](#)[▶I](#)[◀](#)[▶](#)[Back](#)[Close](#)[Full Screen / Esc](#)[Printer-friendly Version](#)[Interactive Discussion](#)

SECHIBA forced by NLDAS

M. Guimberteau et al.

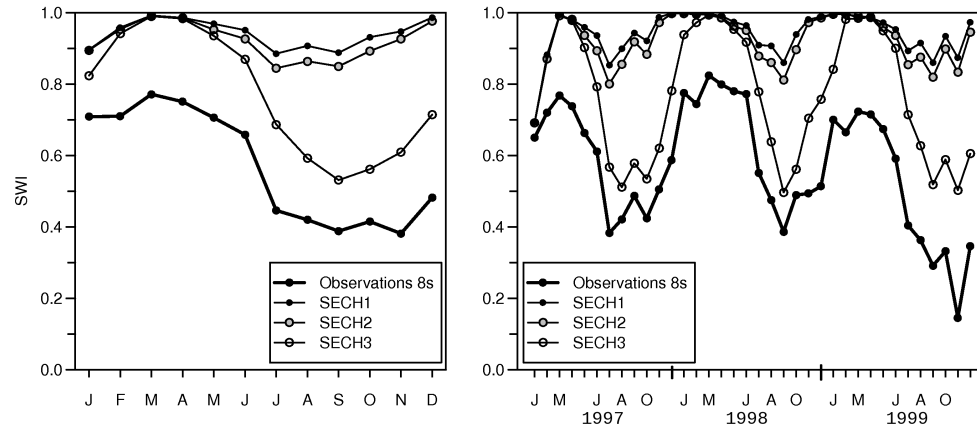


Fig. 6. Monthly mean SWI averaged over the eight selected stations, from observations and simulations SECH1 to SECH3. **(a)** Averaged seasonal cycles and **(b)** time series over the time period 1997–1999.

[Title Page](#)
[Abstract](#)
[Introduction](#)
[Conclusions](#)
[References](#)
[Tables](#)
[Figures](#)
[◀](#)
[▶](#)
[◀](#)
[▶](#)
[Back](#)
[Close](#)
[Full Screen / Esc](#)
[Printer-friendly Version](#)
[Interactive Discussion](#)


**SECHIBA forced by
NLDAS**

M. Guimberteau et al.

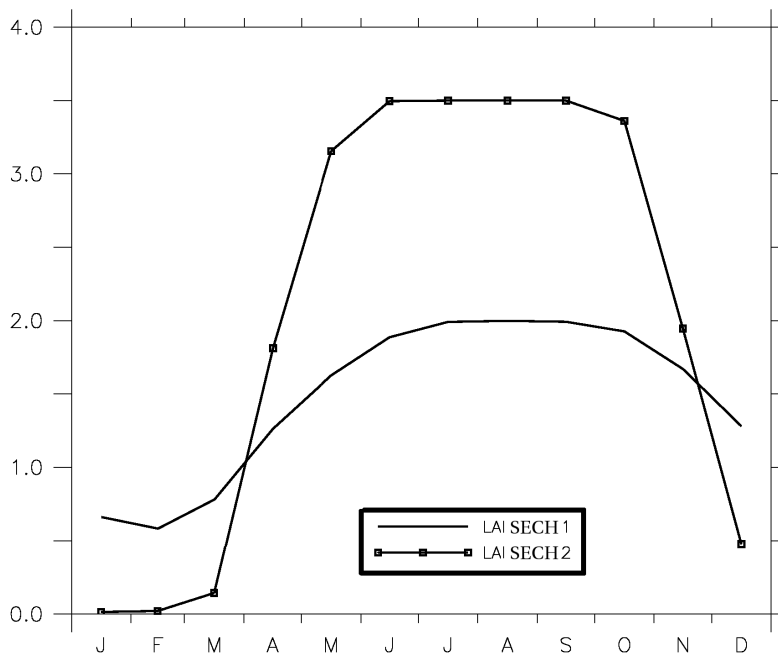


Fig. 7. Seasonal cycles of LAI simulated in SECH1 and SECH2 simulations, in average over the eight selected grid cells, for the mean time period 1997–1999.

[Title Page](#)[Abstract](#)[Introduction](#)[Conclusions](#)[References](#)[Tables](#)[Figures](#)[◀](#)[▶](#)[◀](#)[▶](#)[Back](#)[Close](#)[Full Screen / Esc](#)[Printer-friendly Version](#)[Interactive Discussion](#)

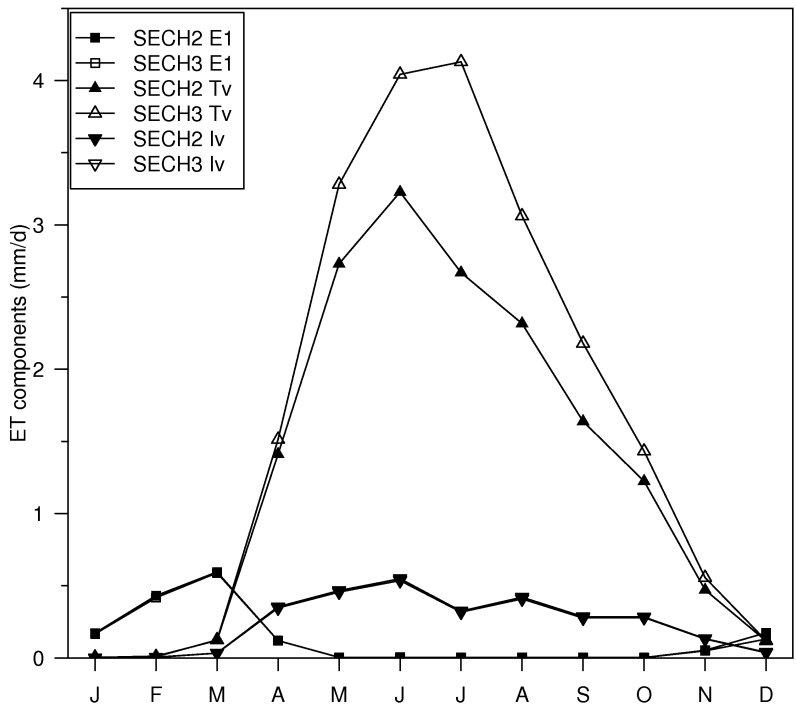


Fig. 8. Seasonal cycles of monthly mean ET components (sublimation not shown) (mm d^{-1}) averaged over the eight selected grid cells, from SECH2 and SECH3, for the mean time period 1997–1999. ET components are E_1 (bare soil evaporation), T_v (transpiration) and I_v (evaporation of water intercepted by the cover).

SECHIBA forced by NLDAS

M. Guimberteau et al.

Title Page

Abstract	Introduction
Conclusions	References
Tables	Figures

◀
▶

◀
▶

Back
Close

Full Screen / Esc

Printer-friendly Version

Interactive Discussion



SECHIBA forced by NLDAS

M. Guimberteau et al.

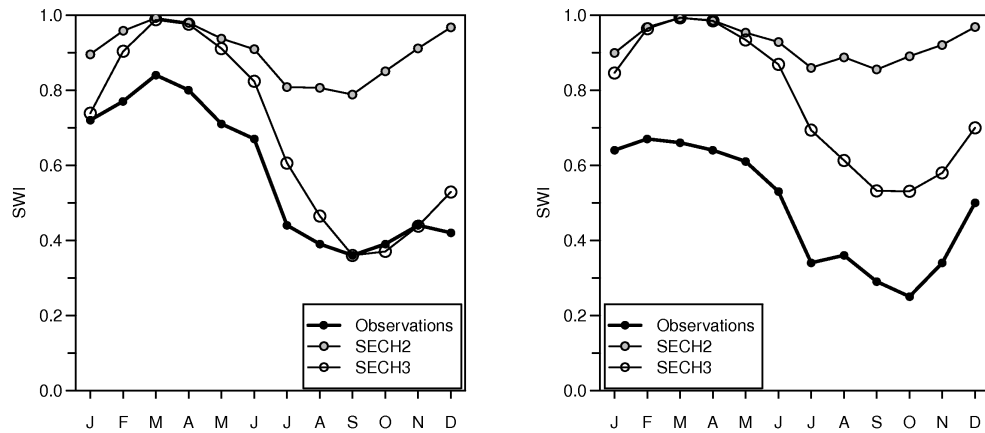


Fig. 9. Seasonal cycles of monthly mean SWI on (a) station 9 and (b) station 16, from observations and simulations SECH2 and SECH3, for the mean time period 1997–1999.

[Title Page](#)
[Abstract](#) [Introduction](#)
[Conclusions](#) [References](#)
[Tables](#) [Figures](#)
[I◀](#) [▶I](#)
[◀](#) [▶](#)
[Back](#) [Close](#)
[Full Screen / Esc](#)
[Printer-friendly Version](#)
[Interactive Discussion](#)



SECHIBA forced by NLDAS

M. Guimberteau et al.

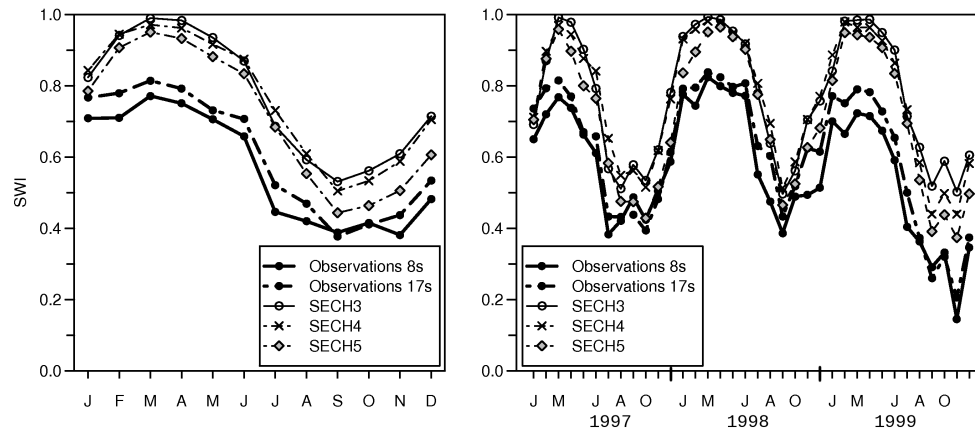


Fig. 10. Monthly mean SWI averaged over all the stations, from observations and SECH3 to SECH5. **(a)** Averaged seasonal cycles and **(b)** time series over the time period 1997–1999.

Title Page

Abstract

Introduction

Conclusions

References

Tables

Figures

◀

▶

◀

▶

Back

Close

Full Screen / Esc

Printer-friendly Version

Interactive Discussion



SECHIBA forced by NLDAS

M. Guimberteau et al.

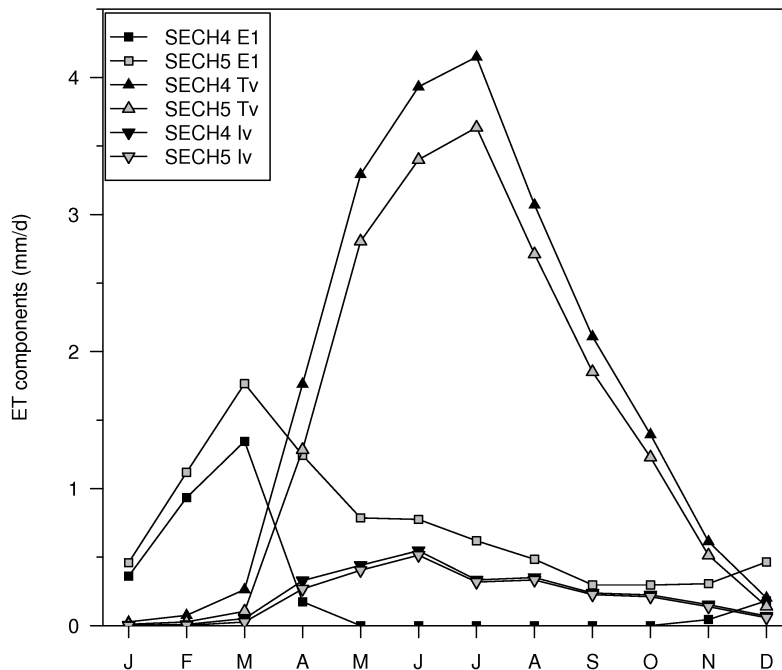


Fig. 11. Seasonal cycles of monthly mean ET components (sublimation not shown) (mm d^{-1}) averaged over all the selected grid cells, from SECH4 and SECH5, for the mean time period 1997–1999. ET components are E_1 (bare soil evaporation), T_v (transpiration) and l_v (evaporation of water intercepted by the cover).

Title Page

Abstract

Introduction

Conclusions

References

Tables

Figures

◀

▶

◀

▶

Back

Close

Full Screen / Esc

Printer-friendly Version

Interactive Discussion



SECHIBA forced by NLDAS

M. Guimberteau et al.

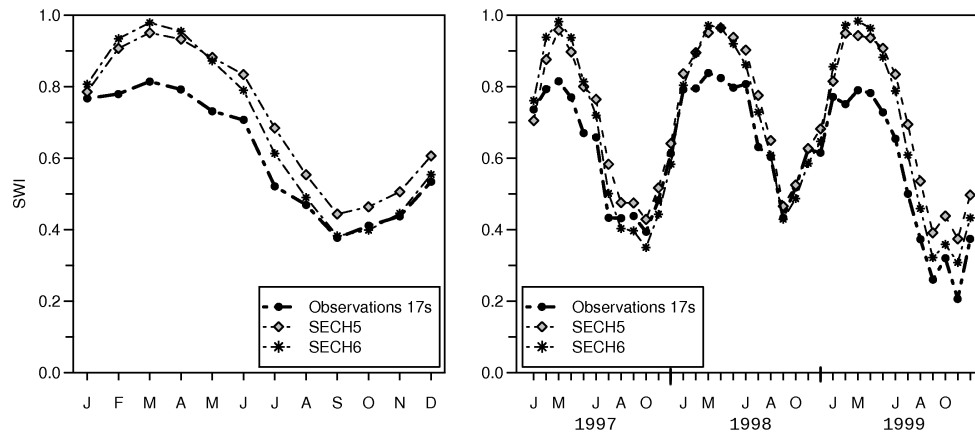


Fig. 12. Monthly mean SWI averaged over all the stations, from observations, SECH5 and SECH6. **(a)** Averaged seasonal cycles and **(b)** time series over the time period 1997–1999.

Discussion Paper | Discussion Paper | Discussion Paper | Discussion Paper

[Title Page](#)
[Abstract](#) [Introduction](#)
[Conclusions](#) [References](#)
[Tables](#) [Figures](#)
[◀](#) [▶](#)
[◀](#) [▶](#)
[Back](#) [Close](#)
[Full Screen / Esc](#)
[Printer-friendly Version](#)
[Interactive Discussion](#)



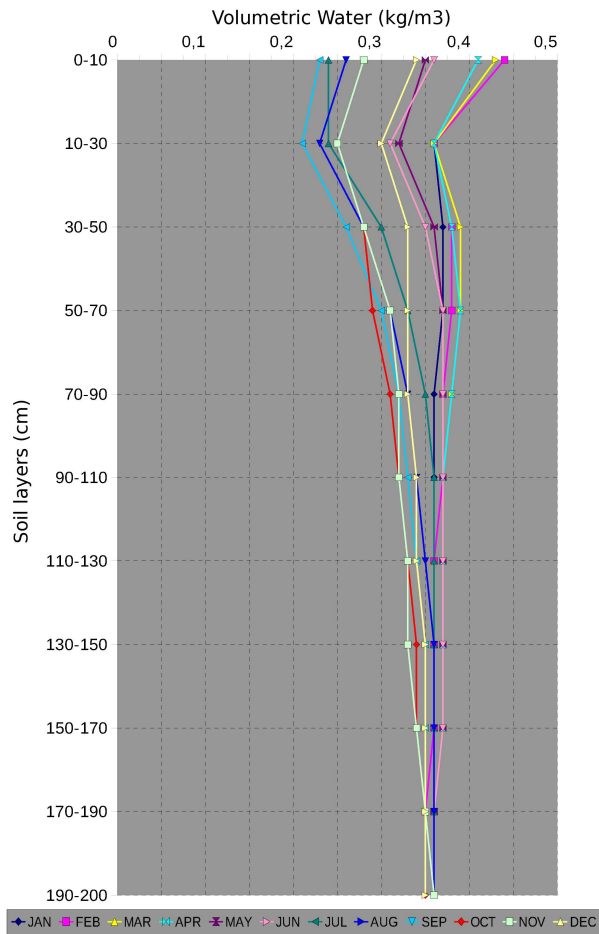


Fig. 13. Monthly mean volumetric water profiles averaged over all the stations, for the mean time period 1997–1999.

SECHIBA forced by NLDAS

M. Guimberteau et al.

Title Page

Abstract Introduction

Conclusions References

Tables Figures

◀ ▶

◀ ▶

Back Close

Full Screen / Esc

Printer-friendly Version

Interactive Discussion



SECHIBA forced by
NLDAS

M. Guimberteau et al.

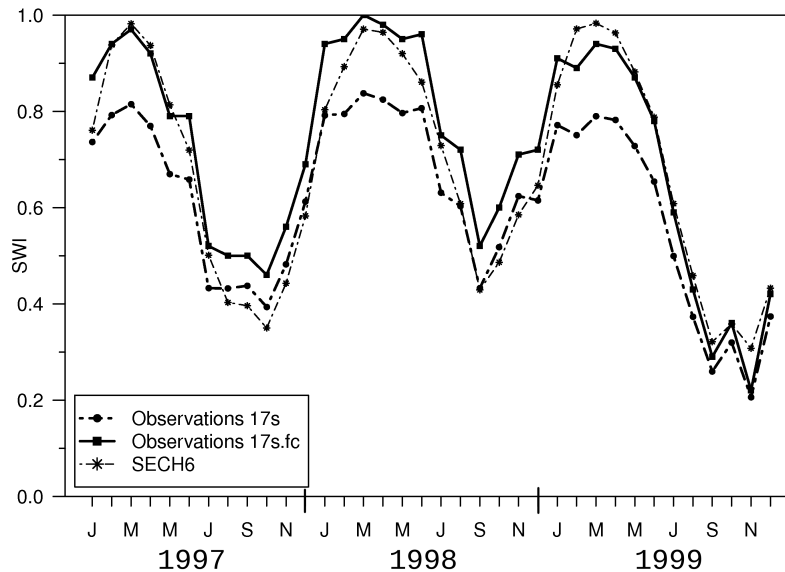


Fig. 14. Times series of monthly mean SWI averaged over all the stations, from observations, new profile of observations and SECH6, for the time period 1997–1999.

[Title Page](#)[Abstract](#)[Introduction](#)[Conclusions](#)[References](#)[Tables](#)[Figures](#)[I◀](#)[▶I](#)[◀](#)[▶](#)[Back](#)[Close](#)[Full Screen / Esc](#)[Printer-friendly Version](#)[Interactive Discussion](#)

SECHIBA forced by NLDAS

M. Guimberteau et al.

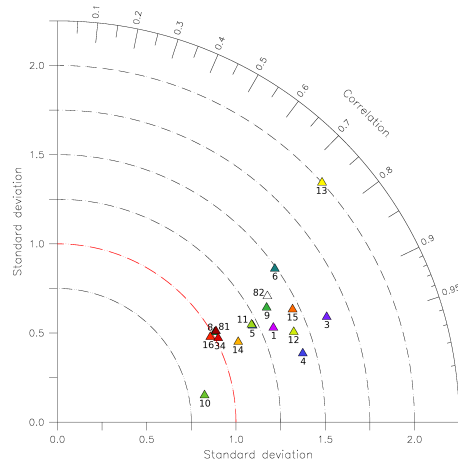


Fig. 15. Taylor diagram illustrating the statistics of SWI simulated with SECH6, from 1997 to 1999. Each station is represented by a colored triangle with its number. The Taylor diagram is a representation that provides the ratio of the simulated and the observed standard deviation as a radial distance from the origin and the correlation of simulated SWI with observations as the cosine of the azimuth angle in a polar plot. R correlation coefficient is computed according to the following equation: $R = \frac{\frac{1}{N} \sum_{n=1}^N (Q_n^{\text{ORCH}} - Q^{\text{ORCH}})(Q_n^{\text{OBS}} - Q^{\text{OBS}})}{\sigma_{Q^{\text{ORCH}}} \sigma_{Q^{\text{OBS}}}}$ where n is the month ($1 < n < N = 36$), Q^{ORCH} and Q^{OBS} are, respectively simulated and observed monthly mean SWI and $\sigma_{Q^{\text{ORCH}}}$ and $\sigma_{Q^{\text{OBS}}}$ are, respectively simulated and observed standard deviations. The mean SWI averaged over all the stations is plotted at (1,0): no error in standard deviation and zero correlation error. The distance between the point (1,0) and the simulated result point is proportional to the root mean squared error. Good representation of the amplitude simulated by the model compared to observations is traduced by a triangle close to the dashed red line as radial distance. Good representation of the phase is traduced by a short distance between the triangle and the unit on the abscissa axis.

Title Page

Abstract

Introduction

Conclusions

References

Tables

Figures

◀

▶

◀

▶

Back

Close

Full Screen / Esc

Printer-friendly Version

Interactive Discussion



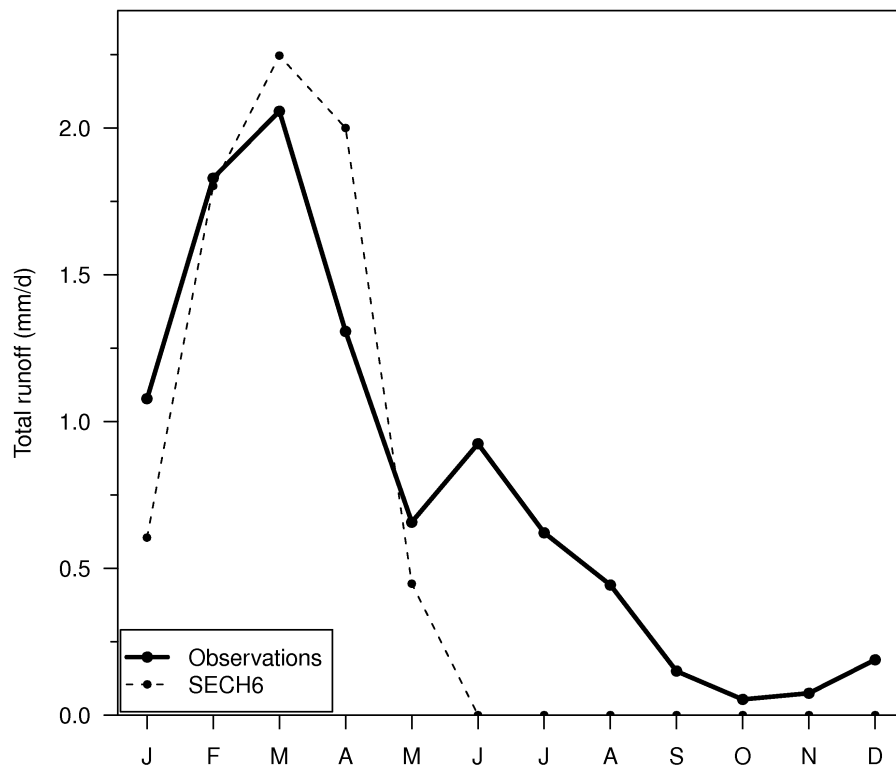


Fig. 16. Seasonal cycles of monthly mean total runoff (mm d^{-1}) on the grid cell corresponding to Venedy station coordinates, from observations and SECH6, for the mean time period 1997–1999.

SECHIBA forced by NLDAS

M. Guimberteau et al.

Title Page	
Abstract	Introduction
Conclusions	References
Tables	Figures
◀	▶
◀	▶
Back	Close
Full Screen / Esc	
Printer-friendly Version	
Interactive Discussion	



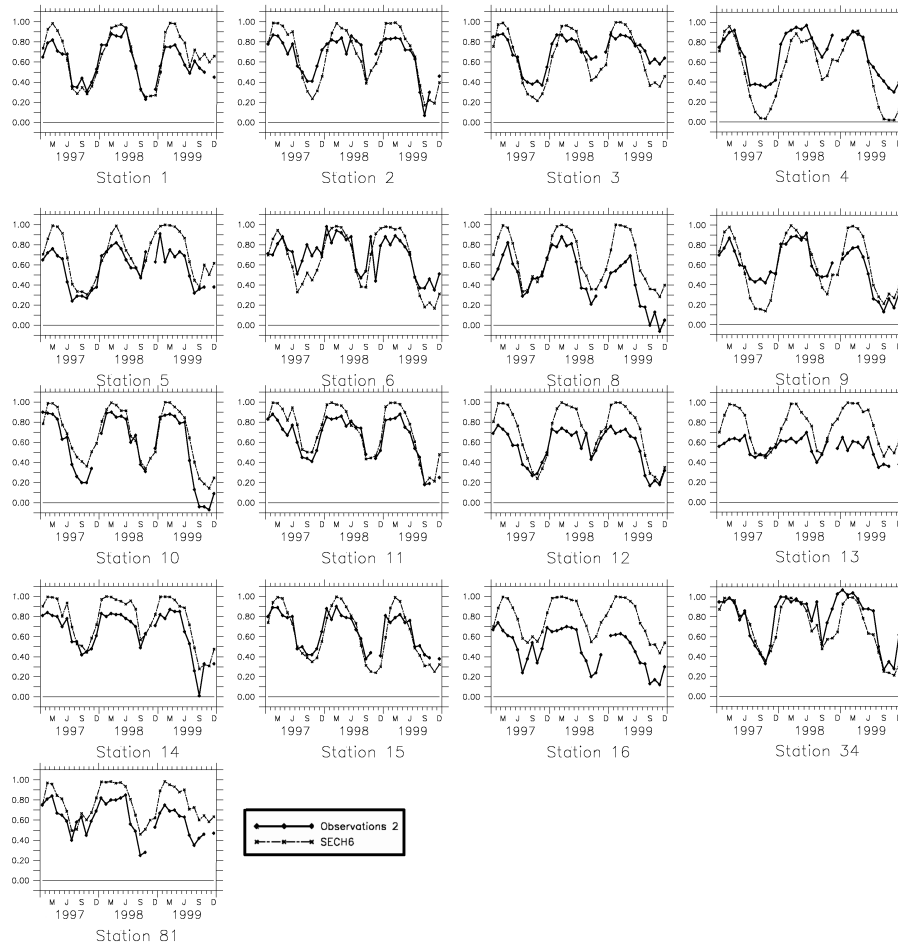


Fig. A1. Times series of monthly mean SWI for each studied stations, from observations and SECH6, for the time period 1997–1999.

Title Page

Abstract Introduction

Conclusions References

Tables Figures

◀ ▶

◀ ▶

Back Close

Full Screen / Esc

Printer-friendly Version

Interactive Discussion

